PRAMANA
— journal of
physics

© Indian Academy of Sciences

Vol. 71, No. 6
December 2008
pp. 1301–1310

# Development of a 2 MW relativistic backward wave oscillator

YADUVENDRA CHOYAL[1,*], LALIT GUPTA[1], PRASAD DESHPANDE[1], KRISHNA PRASAD MAHESHWARI[1], KAILASH CHANDER MITTAL[2] and SURESH CHAND BAPNA[3]

[1]School of Physics, Devi Ahilya Vishwavidyalaya, Indore 452 001, India
[2]Accelerator and Pulse Power Division, Bhabha Atomic Research Centre, Mumbai 400 085, India
[3]D.C. Accelerator Laboratory, Raja Ramanna Centre for Advanced Technology, Indore 452 013, India
*Corresponding author. E-mail: ychoyal@yahoo.com

MS received 13 February 2008; revised 22 May 2008; accepted 17 June 2008

**Abstract.** In this paper, a high power relativistic backward wave oscillator (BWO) experiment is reported. A 230 keV, 2 kA, 150 ns relativistic electron beam is generated using a Marx generator. The beam is then injected into a hollow rippled wall metallic cylindrical tube that forms a slow wave structure. The beam is guided using an axial pulsed magnetic field having a peak value 1 T and duration 1 ms. The field is generated by the discharge of a capacitor bank into a solenoidal coil. A synchronization circuit ensures the generation of the electron beam at the instant when the axial magnetic field attains its peak value. The beam interacts with the SWS modes and generates microwaves due to Cherenkov interaction. Estimated power of 2 MW in $TM_{01}$ mode is observed.

**Keywords.** Backward wave oscillator; high power microwave generation; capacitor charging power supply; relativistic electron beam; Marx generator; high-voltage pulse technology.

**PACS Nos 41.60.Bq; 41.75.-i; 52.59.-f**

## 1. Introduction

Backward wave oscillator (BWO) is one of the devices that efficiently converts energy of an electron beam into electromagnetic radiation at microwave frequencies [1–11]. It essentially consists of an electron beam, confined radially by a strong magnetic field, propagating through a slow wave structure (SWS). The SWS is a rippled wall metallic waveguide having radial profile specified by $R(z) = R_0 + h\cos(k_0 z)$, where $R_0$ is the mean radius, $h$ is the corrugation depth and $z_0 = 2\pi/k_0$ is the spatial periodicity. It provides a set of electromagnetic structure modes having phase velocity less than the velocity of the beam electrons. These slow waves

therefore can interact resonantly with the negative energy slower space charge wave supported by the beam leading to an instability that transfers the energy from the beam to the electromagnetic wave field.

In this paper we present our experimental study of all the major subsystems of the developed BWO. A 230 kV high voltage pulse of 150 ns duration generated from a Marx generator is being fed to a relativistic electron beam (REB) diode. The generated REB, guided by an axial magnetic field, injects into the SWS. The magnetic field is uniform over the time scale of the beam duration and is in the form of a 1 ms half sine pulse having a maximum at 1 T. This field is generated by the discharge of a capacitor bank into a solenoidal coil wound over the SWS. A synchronization circuit ensures triggering of the electron beam at an instant when the axial magnetic field attains its peak value. The SWS–electron beam interaction results in the generation of high power microwaves (HPM). These microwaves are detected using a two-dimensional array of neon gas bulbs and crystal detector. HPM with $\sim$2 MW of power in $TM_{01}$ mode are observed.

## 2. Experimental

Schematic of the experimental set-up is given in figure 1. The major subsystems are: a Marx generator and its power supply synchronized with a capacitor bank for magnetic field generation, REB diode, SWS structure along with a radiating horn antenna. The high voltage capacitors of the Marx generator are charged in parallel and discharged in series resulting in voltage multiplication [12,13]. The present Marx generator can deliver an output voltage pulse, which has a maximum voltage rating of 300 kV on matched load, energy 180 J and pulse duration 150 ns for 30 kV DC charging [14]. There are 20 Marx stages assembled by stacking one over the other in the vertical towering shape. Each stage is made up of one 21 nF capacitor, one spark gap (SG) and two non-inductive resistors having value 50 $\Omega$ each. Capacitor of each stage is charged by a DC power supply (0–30 kV, 20 mA). Capacitor in each module is mounted on a horizontal perspex sheet. The lowest stage has a triggered SG which is closed by a 6 kV pulse obtained with the help of a pulse transformer. SGs in each stage are aligned in line-of-sight so that the UV emitted from the first triggered SG can cause pre-ionization of the remaining gaps to ensure reliability in the simultaneous sparking of all the gaps by reducing the statistical time lag. All the stages are held together by a perspex casing having dimensions of 28 cm $\times$ 28 cm $\times$ 150 cm and mounted on a 10 mm thick aluminum plate supported on wheels. The entire Marx assembly is kept in a metallic case for EMI shielding.

The high voltage terminal of the Marx generator is connected to REB diode. The geometry of REB diode is as follows: A 50 cm long, 10 mm diameter stainless steel (SS) rod is insulated by epoxy casting. The outer surface of the insulator is rippled to inhibit surface flash-over. The structure is then placed inside a hollow SS cylinder $C_1$ of 25 cm inner diameter and is kept at ground potential. One end of the SS rod is connected to different types of cathodes like aluminum, brass, SS, velvet and graphite cathodes, while the other end joins to the high voltage end of the Marx generator. Length of the cathode is 8.6 cm and diameter is 1.5 cm. A

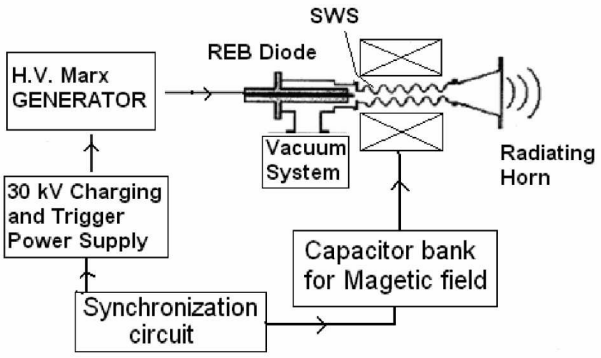


**Figure 1.** Schematic of the BWO experiment.

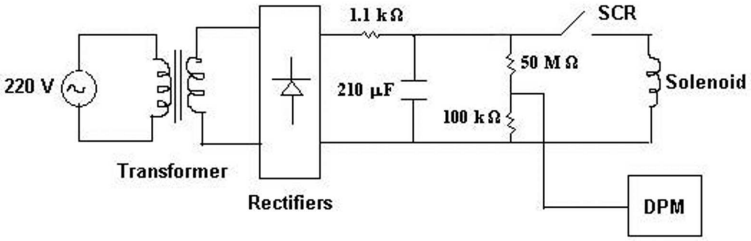


**Figure 2.** Schematic of power supply.

blank disc is connected to one end of $C_1$. The gap between the cathode and the disc can be varied from 6 to 12 mm. This geometry forms a planar diode. The air is evacuated to a pressure of $2 \times 10^{-5}$ Torr. Beam voltage is measured by introducing shielded voltage divider between input to cathode and the ground.

For the BWO experiment, it is important that a well-focused electron beam is injected into the interaction region. However, the main limitation for the intense beam transport is the electrostatic potential depression that results from the electron beam space charge [15]. This electrostatic potential not only expands the beam, but it can even reflect the beam if it is sufficiently strong. The beam transport is hampered if the injected beam current exceeds the space charge limiting current of the guide cavity due to a virtual cathode formation. The beam transport is accomplished using sufficiently high axial magnetic field. The necessary condition for the stable equilibrium transport of the beam is $\Omega^2 > 2\omega_e^2/\gamma$, where $\Omega$ is the electron cyclotron frequency, $\omega_e$ is the beam electron plasma frequency, and $\gamma$ is the relativistic factor of the electron beam. We have developed pulsed synchronized magnetic field for the propagation of the unneutralized electron beam. The schematic of the power supply is depicted in figure 2. Magnetic field pulse of peak value 1 T and duration 260 $\mu$s over an axial length of 20 cm (Type 1) and 1 ms over 12 cm length (Type 2) is generated using this supply.

A schematic of a rippled wall SWS is shown in figure 3. One end is the cut-off for the waveguide eigenmodes while the other is the radiating end. Our present SWS consists of eight periods, each period being fabricated in pieces [16]. All the

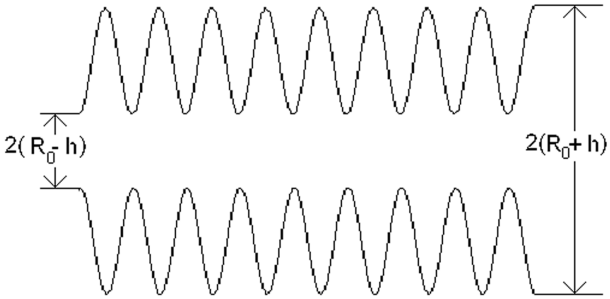


**Figure 3.** Schematic of the slow wave structure.

pieces are then stacked together. A uniform wall thickness of 3 mm is maintained so that magnetic field diffuses uniformly into the resulting waveguide. The assembly is placed into a cylinder for mechanical stability and vacuum. The parameters of the SWS are $R_0 = 1.5$ cm, $h = 0.5$ cm, $z_0 = 1.5$ cm. The length of the SWS is therefore 12 cm. The parameters are optimized for 8 GHz microwaves at $\pi$ point interaction by analysing the dispersion relation of BWO excited by 300 kV electron beam.

The REB when passed through the BWO generates HPM by Cherenkov interaction. The high power microwaves are then radiated out with the help of the radiating horn antenna. A two-dimensional neon gas lamp array is placed against the radiating horn for mode pattern and power estimate [17,18]. Microwaves are also detected using a crystal detector.

## 3. Results and discussion

A 230 kV Marx voltage pulse is applied to the cathode of the REB diode. The voltage across the beam, after scaling down by a factor of 1000 by $CuSO_4$ shielded voltage divider is further attenuated by a factor of 100 using Tektronics voltage attenuators at the oscilloscope end. The attenuated signal is then fed to a 100 MHz digital storage oscilloscope (TDS 220, Tektronics). A typical beam voltage waveform for 7.5 mm cathode–anode gap of the REB diode is shown in figure 4. A maximum pulse voltage of ∼160 kV together with a voltage reversal of 10 kV is observed. The signal shows an initial narrow (∼10 ns) burst in voltage, after which the expected pulse shape is obtained. During the rise of voltage in this burst, the cathode–anode gap is open as the plasma has not yet formed. As soon as plasma is formed in the gap, the impedance starts collapsing and reaches a steady value of $R_{\mathrm{REB}} = 90\ \Omega$. The beam voltage is therefore obtained after ignoring the initial narrow pulse.

For the transportation of the electron beam through the SWS of BWO it is necessary to have a constant and uniform magnetic field over the electron pulse duration. The magnetic field is half sine pulse of 260 $\mu$s duration for the Type-1 solenoid. A synchronization circuit ensures that the Marx generator is erected when the magnetic field pulse attains a maximum. This result is shown in figure 5.

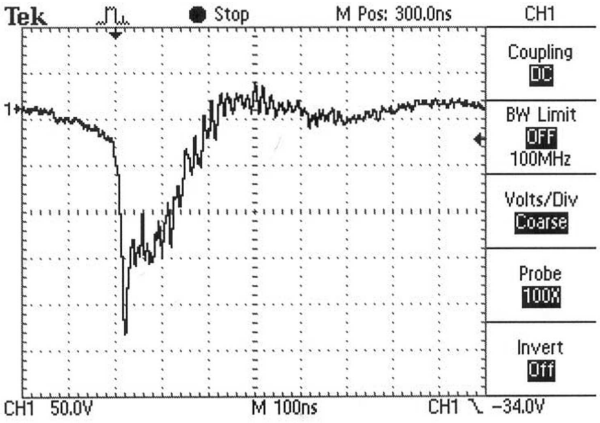


**Figure 4.** Beam voltage waveform.

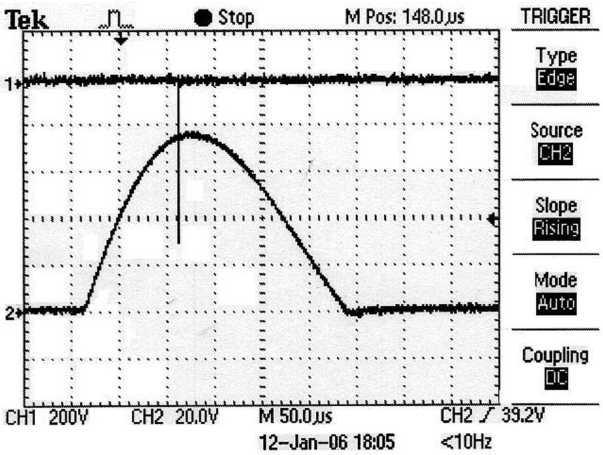


**Figure 5.** Synchronization of beam voltage and magnetic field pulse. Channel 1 depicts the beam. Channel 2 depicts the magnetic field.

Channel 1 depicts the electron beam voltage after the scaling as done in figure 4. Channel 2 depicts the integrated voltage of a search coil of radius 5 mm. The coil is of 7 turns. Once calibrated, the voltage measured is equivalent to the measurement of magnetic field. It is evident that on the time scale of the electron beam pulse, the magnetic field pulse of duration $\sim$260 $\mu$s appears to be of constant value.

The magnetic field penetration into a drift tube is dependent on the drift tube material and the frequency of the field. The pulsed magnetic field has high as well as low frequency Fourier components. While the low frequency components can penetrate the metallic wall, the high frequency components are attenuated. This broadens and decreases the effective field inside the drift tube. Several studies are made related to magnetic field diffusion through the walls of different metallic drift tubes. The results are depicted in figure 6. The peak magnetic field pulse of the air

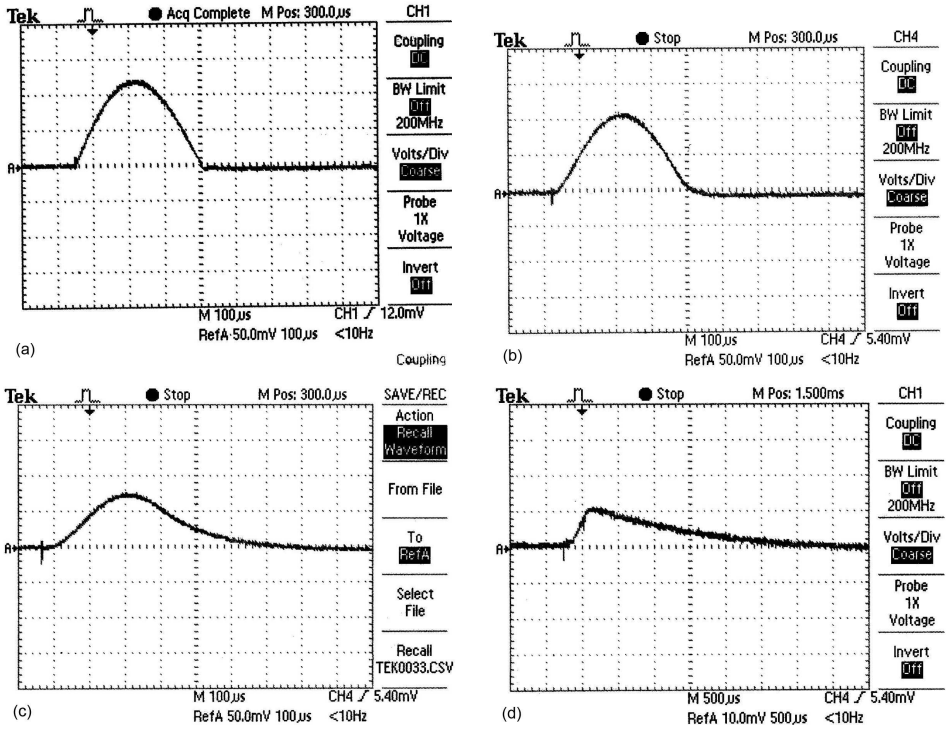


**Figure 6.** Temporal profile of magnetic field pulse at the centre of the solenoid having (**a**) air core, (**b**) 3 mm thick SS tube, (**c**) 9 mm thick SS tube, and (**d**) 3 mm thick copper tube.

core solenoid is taken to be 1 T as shown in figure 6a. When a 3 mm thick stainless steel (SS) drift tube of inner diameter 40 mm is inserted in the solenoid, the field inside the tube gets reduced to 87%. The result is shown in figure 6b. Magnetic field temporal profile at the centre of the tube for 9 mm thick SS tube placed inside the solenoid is shown in figure 6c. In this case, the field strength is reduced to 63% and the pulse gets broadened to 500 $\mu$s showing low frequency component penetration. In figure 6d, magnetic field temporal profile at the centre of the tube for 3 mm thick copper tube is shown. A dramatic twelve-times reduction in magnitude of the field is observed.

Investigation on the beam transport into a 20 cm long, 3 mm thick SS drift tube of inner diameter 40 mm are done observing the impression made on a thermal paper by the energetic beam electrons. The location of the thermal paper, i.e., the screen can be varied inside the drift tube. All the distances are measured from the input end of the drift tube. Results are depicted in figure 7. The solid/annular spot is the beam impression. The beam is solid having radial density variation. It is most intense at the centre, and therefore it completely burns the thermal paper. Therefore, all the spots are essentially due to solid beam. In figures 7a–d, strength of the magnetic field is 1 T. Figures 7a, 7e, and 7i are for spots at a distance 5 cm. Figures 7b, 7f, and 7g show the spot size at a distance of 10 cm. The case for the

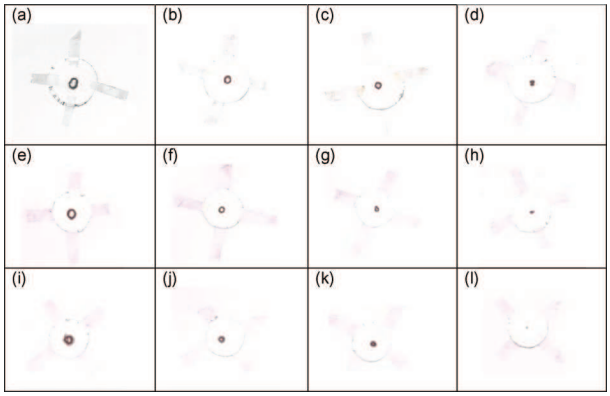


**Figure 7.** Electron beam spots in drift tube. The charging voltage for the Marx generator is 15 kV. The guide magnetic field at the centre of the drift tube for (**a**)–(**d**) is 1 T, for (**e**)–(**h**) is 0.75 T, and for (**i**)–(**l**) is 0.5 T. The drift distances for (a), (e), and (i) are 5.0 cm, for (b), (f), and (j) are 10 cm, for (c), (g), and (k) are 15.0 cm, and for (d), (h), and (l) are 20 cm.

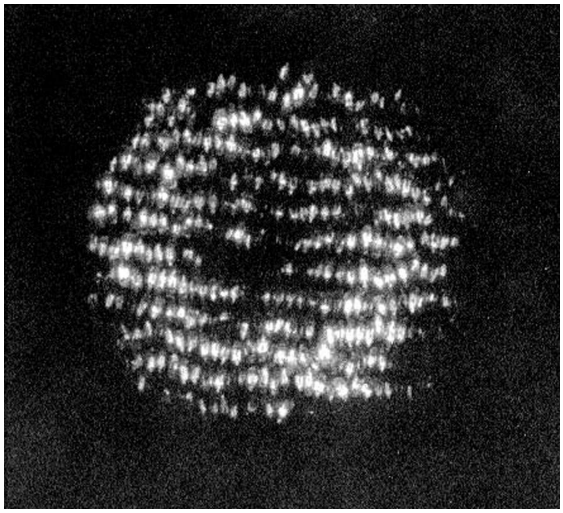

**Figure 8.** HPM-induced gas breakdown pattern in two-dimensional array of neon bulbs placed 10 cm from the radiating horn.

distance 15 cm is shown in figures 7c, 7f, and 7j. The final set of figures 7d, 7g, and 7l are the spots at the exit end of the solenoid. Radii of the beam at 5, 10, 15, and 20 cm for 1 T field are 4, 2, 1.5, and 0.75 mm. As in a solenoid the magnetic field at the ends is half the field at centre, the beam initially gets compressed till it reaches the middle of drift tube. Then it again expands. The beam electrons are however lost due to collision with low pressure air molecules present in the tube and so the thermal spot gets smaller and the white portion at the centre depicting intense beam gets reduced.

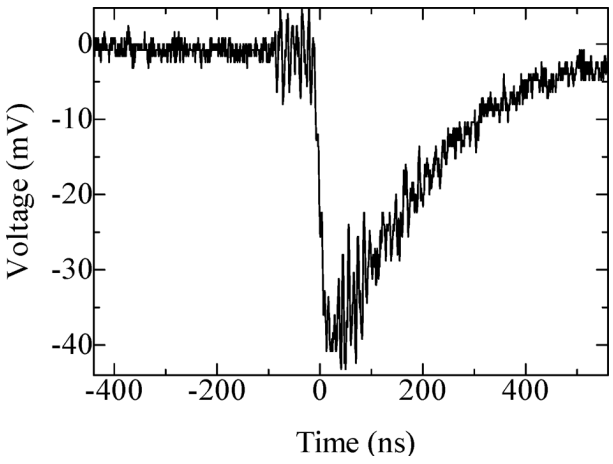


**Figure 9.** Signal from the microwave crystal detector that detected radiation from the radiating horn.

Figure 8 depicts the glow induced in the gas of a two-dimensionally arranged neon flash lamps by microwaves. The neon glow is typically induced when >5 kW of microwave power impinges on 1 $cm^2$ area of the glow bulbs. Theoretical study of pulsed microwave discharge at low pressure nitrogen has been carried out by Bonaventura *et al* [19]. In the presence of an applied harmonic electric field of magnitude $E_0 \cos(\omega t)$, electron concentration in a low pressure neon gas can be calculated by the equation

$$\frac{\mathrm{d}n_\mathrm{e}}{\mathrm{d}t} = n_\mathrm{e}(N\langle k_\mathrm{t}\rangle - \langle v_\mathrm{d}\rangle),$$

where $N$ is the gas density, $n_\mathrm{e}$ is the electron density, $\langle k_\mathrm{t}\rangle$ is the time-averaged ionization coefficient, and $\langle v_\mathrm{d}\rangle = \langle D\rangle/\Lambda^2, \langle D\rangle$ being the time-averaged diffusion coefficient and $\Lambda$ is the diffusion length. Here, both $\langle k_\mathrm{t}\rangle$ and $\langle v_\mathrm{d}\rangle$ are functions of $E_0$. The breakdown electric field $E_\mathrm{b}$ can be obtained from the relation

$$N\langle k_\mathrm{t}\rangle(E_\mathrm{b}) = \langle v_\mathrm{d}\rangle(E_\mathrm{b}).$$

From $n_\mathrm{e}$, $E_\mathrm{b}$, and $\langle v_\mathrm{d}\rangle$, the density of microwave power absorbed in the plasma, i.e., $\mathbf{j}\cdot\mathbf{E}$ can be obtained. Bonaventura *et al* have obtained that 200 ns pulsed microwaves induce breakdown in low pressure nitrogen at $E_\mathrm{b} = 1.67$ kV/cm. The computed absorbed power density comes out to be 3.3 kW/$cm^2$. As the ionization coefficient for neon is higher than nitrogen, we have taken power density to induce the breakdown of neon gas as approximately 5 kW/$cm^2$. In our experiment, the area of the glowed neon array was 380 $cm^2$, implying that at least 2 MW of microwave power in X band in $TM_{01}$ mode is radiated by the BWO. Microwave intensity decreases with distance and gas breakdown is barely visible 25 cm away from the antenna. A black paper on the radiating horn ensures that no optical radiation emanating from the cathode–anode plasma in the diode region or the beam produced plasma in the SWS region is recorded. It has been confirmed that the microwave-induced glow stops if an aluminum foil is wrapped on the radiating

antenna. The power can be increased by placing the beam near the SWS wall and increasing the $Q$ factor of the waveguide. In our first experiment, the variation of power as a function of $Q$ factor of the SWS was not calculated and these questions are left out for further exploration in future.

Microwaves were also detected by crystal detector Model 503A (NARDA, USA). A double-ridged horn model 3115 (ETS Lindgren, USA) having a gain of 10 dB for 8 GHz is placed 5.7 m away from the radiating horn collects microwaves. The signal is then attenuated by 30 dB using attenuator Model 776C-30 (NARDA, USA). Figure 9 depicts the microwave signal detected by crystal detector. Peak voltage signal of 1.6 mV corresponds to 10 dbm or 10 mW of microwave power incident on the crystal detector. Attenuator and the free space loss (FSL) given by the expression FSL = 20 $\log_{10}(d)$ + 20 $\log_{10}(f)$ − 147.55 dB, where $d$ is the distance between radiating and receiving horns and $f$ is the frequency in Hz, results in total attenuation of 85.63 dB. This implies power level of 3.65 MW. The power however is less than this value because the FSL is for isotropic radiation whereas BWO radiates in a cone.

In summary, a full BWO experiment is carried out. All the subsystems have been designed and developed locally. Microwave power of 2 MW in $TM_{01}$ mode is observed. Further experiments will be carried out to optimize the BWO device for higher emitted HPM power.

## Acknowledgments

The authors thank Dr Lalit Kumar, Microwave Tube Research and Development Centre, Bangalore, India for his useful comments and inputs. Financial assistance by Defence Research and Development Organization, New Delhi, India is gratefully acknowledged. YC is thankful to Prof. K Minami, Department of Electrical and Electronic Engineering, Niigata University for his discussions.

## References

[1] R J Barker and E Schamiloglu, *High-power microwave sources and technologies* (IEEE Press, New York, 2001)
[2] Y Carmel, J Ivers, R E Kribel and J Nation, *Phys. Rev. Lett.* **33**, 1278 (1974)
[3] V I Kurilko, V I Kucherov, A O Ostrovskii and Yu V Tkach, *Sov. Phys. Tech. Phys.* **24**, 1451 (1979)
[4] L S Bogdankevich, M V Kuzelev and A A Rukhadze, *Sov. Phys. Usp.* **24**, 1 (1981)
[5] J A Swegle, J W Poukey and G T Leifeste, *Phys. Fluids* **28**, 2882 (1985)
[6] R A Kehs, A Bromborsky, G B Ruth, S E Graybill, W W Destler, Y Carmel and M C Wang, *IEEE Trans. Plasma Sci.* **13**, 559 (1985)
[7] K Minami, W R Lou, W W Destler, R A Kehs, V L Granatstein and Y Carmel, *Appl. Phys. Lett.* **53**, 559 (1988)
[8] Y Carmel, W R Lou, T M Antonsen Jr, J Rodgers, B Levush, W W Destler and V L Granatstein, *Phys. Fluids* **B4**, 2286 (1992)
[9] Y Choyal and K P Maheshwari, *Phys. Plasmas* **1**, 171 (1994)
[10] K Tanaka, K Minami and T Nagahama, *J. Phys. Soc. Jpn.* **67(11)**, 3779 (1998)

[11] K Minami, M Saito, Y Choyal, K P Maheshwari and V L Granatstein, *IEEE Trans. Plasma Sci.* **30**, 1134 (2002)
[12] P H Ron, *Private lecture notes on high power pulse technology* (1993) (unpublished)
[13] K C Mittal, *Gigawatt pulsed relativistic electron beam generation studies in vacuum and gas-filled diodes*, Ph.D. Dissertation (University of Bombay, Mumbai, 1986) (unpublished)
[14] Y Choyal, L Gupta, P Vyas, P Deshpande, A Chaturvedi, K C Mittal and K P Maheshwari, *Sadhana* **30**, 757 (2005)
[15] R B Miller, *An introduction to the physics of intense charge particle beams* (Plenum, New York, 1982)
[16] K Tanaka, K Minami, X Zheng, Y Carmel, A N Vlasov and V L Granatstein, *IEEE Trans. Plasma Sci.* **26**, 940 (1998)
[17] V L Granatstein and I Alexeff, *High power microwave sources* (Artech House, Boston, 1987)
[18] P Felsental and J M Proud, *Phys. Rev.* **139**, A1796 (1965)
[19] Z Bonaventura, D Trunec, M Mesko, P Vasina and V Kudrle, *Plasma Source Sci. Technol.* **14**, 751 (2005)